JOURNAL OF MATERIALS SCIENCE 15 (1980) 1371–1378

Sintering of optical wave-guide glasses

M. F. YAN, J. B. MACCHESNEY, S. R. NAGEL, W. W. RHODES
Bell Laboratories, Murray Hill, New Jersey 07974, USA

Sintering kinetics of glasses prepared by external vapour-deposition technique were quantitatively measured at temperatures ranging from 1000 to 1390° C. Sintering kinetics of borosilicates are consistent with the model proposed for the viscous flow sintering mechanism. The magnitude and the activation energy of the viscosity data derived from the sintering data agree reasonably well with the published data in the borosilicate system. From the viscosity data and sintering model, the decrease in sintering temperature per unit change in dopant content is calculated. It is also shown that at a certain compositional range, an increase in the dopant content can actually alleviate the problem of bubble growth while maintaining the same sintering conditions. This study can be used to determine the relative composition–time–temperature relations for sintering borosilicate glasses. Thus, it has direct applicability to the sintering of soot forms prepared by the external vapour-deposition technique. Furthermore, because of the similarity in microstructures of glasses prepared by the external vapour-deposition and the MCVD processes, one can anticipate similar sintering kinetics for MCVD preforms.

1. Introduction

Glass preforms for optical waveguides are currently produced by either of two methods, MCVD [1] or external vapour deposition [2]. The rate-limiting step in the manufacturing process is believed to be the consolidation of the as-deposited particles to form a vitreous and pore-free glass. The consolidation step has been identified as a sintering process [3, 4].

Recently, Scherer [5] extended the work of Frenkel [6], Mackenzie and Shuttleworth [7] to derive the sintering kinetics of glass particles by the viscous flow mechanism. Upon the basis of microstructural evidences, it has been concluded that the layer of particles formed on the inner wall of the tube during MCVD is consolidated by sintering [3]. However, the limitations of the specimen size and geometry, and the fact that a thin layer of glass is deposited on the inner wall of a glass tube, make it difficult to study the sintering kinetics quantitatively. Recently, a new technique has been used to deposit the glass particles on an aluminium mandrel by external vapour deposition. Because of the difference in the thermal expansion coefficients of aluminium and glass, the preform is easily removed from the mandrel for study.

The microstructures of the partially sintered glass particles prepared by the MCVD process and by the external vapour-deposition technique are rather similar, as shown in Fig. 1. For the purpose of this study the preform prepared by the latter technique is relatively easy to handle. Thus, glass prepared by this method was used to determine quantitative sintering data. However, these data should also be useful in understanding the consolidation step in the MCVD process. In this study, the sintering data obtained were used to quantitatively verify the viscous flow mechanism. The viscosity values derived from the sintering data were then compared with published data in the SiO_2–B_2O_3 system. From these results there emerges a quantitative picture of the consolidation phenomenon taking place in the MCVD process.

2. Experimental details

A mixture of $SiCl_4$ and BCl_3 vapours in an oxygen carrier gas was reacted in a flame hydrolysis burner to produce particulate oxides which were then deposited on an aluminium mandrel. An

0022–2461/80/061371–08$02.80/0

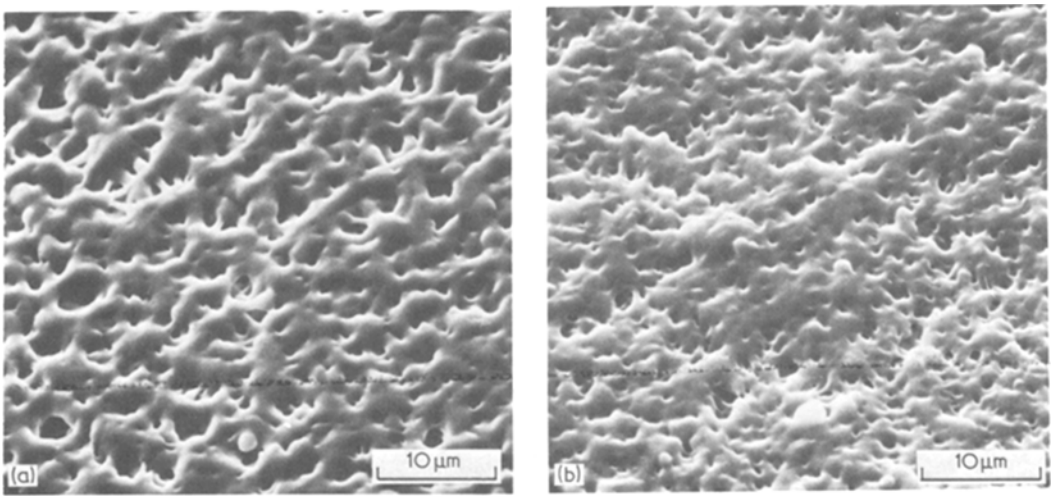

Figure 1 Microstructures of partially sintered glass particles prepared by the MCVD process (a) and by the external vapour deposition technique (b) are shown to be rather similar.

oxide layer about 30 cm long and 0.5 cm thick was formed on a tapered mandrel of ~ 1.74 cm diameter. The oxide shell separated from the mandrel upon cooling and was removed. From the flow rates of $SiCl_4$ and BCl_3, the glass in this study is estimated to have a nominal composition of 6 wt % B_2O_3.

The oxide shell was removed from the mandrel after cooling and sections were sintered in a furnace with a 6 cm hot zone maintained within 2° C of the set point. A flow of helium at a velocity of ~ 0.5 cm sec^{-1} was maintained in the mullite furnace tube. Each specimen was heated to ~ 800° C for 10 min before it was pushed into the hot zone for sintering. After a specific time, the specimen was quenched to the ambient atmosphere during cooling.

Selected specimens were coated with sputtered gold and the microstructures were observed in a scanning electron microscope*.

The bulk density of the sintered preform specimen was measured by submersion in commercial diesel oil following the ASTM standard technique [8]. The density of the diesel oil was 0.850 g cm^{-3} and did not vary more than 0.3% even after the vacuum treatments used during these density measurements.

3. Results and discussion

Sintering kinetics of boron-doped SiO_2 glasses at temperatures ranging from 1000 to 1390° C are reported as relative densities versus sintering time (Fig. 2). It can be observed that the sintering rate rapidly increases with temperature and

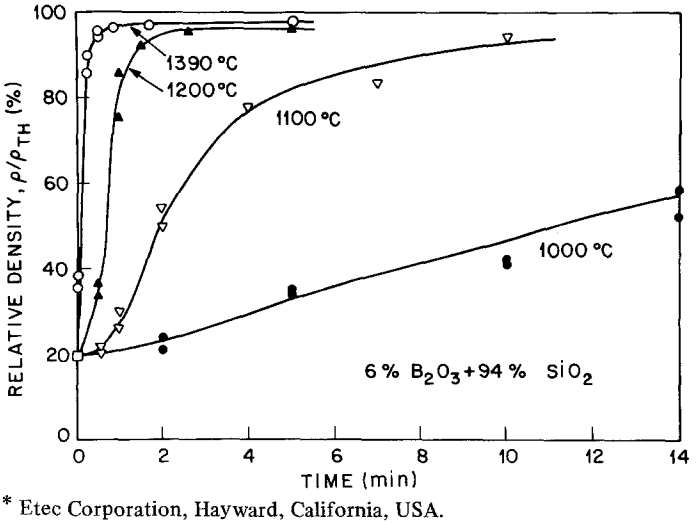

Figure 2 Sintering kinetics of 6% B_2O_3 doped SiO_2 glass at temperatures ranging from 1000 to 1390° C are reported as relative densities versus sintering time.

* Etec Corporation, Hayward, California, USA.

negligible sintering can be expected at temperatures below 1000° C. The densification rate, furthermore, is a strong function of the sintered density and decreases as a specimen approaches the theoretical density. For instance, at temperatures $\geqslant 1200°$ C, the densification rate of a 95% dense specimen is ~ 100 times slower than that of a 20 to 80% dense specimen.

From the scanning electron micrographs on a series of samples, a characteristic microstructure was seen to develop as a function of sintering time as shown in Fig. 3. At low densities, glass particles form a loose interconnected network. During sintering, the array shrinks as glass particles make contact.

All sintering models of glass assume that viscous flow is the mass transport mechanism. During sintering, the reduction in the surface energy is balanced by the energy dissipated in viscous flow. Kinetic equations can be derived based on this energy balance concept [5–7]. Scherer [5] derived such a sintering equation with a specific consideration for a cubic array formed by intersecting glass cylinders, which is a reasonable approximation for the geometry of the particle network in glass preforms observed in this study. The analytic equation relating the sintering time and density is given as

$$K(t-t_0) = \int_0^x \frac{2\,dx}{x^{2/3}(3\pi - 8\sqrt{2}x)^{1/3}} \quad (1)$$

where

$$x \equiv a/l \quad (2)$$

$$\rho/\rho_{TH} \equiv 3\pi x^2 - 8\sqrt{2}x^3, \quad (3)$$

$$K \equiv \frac{\gamma}{\eta l_0}\left(\frac{\rho_{TH}}{\rho_0}\right)^{1/3} \quad (4a)$$

γ is the surface energy, η is the viscosity, ρ is the sintered density, ρ_{TH} is the theoretical density, a and l are radius and length, respectively, of the glass cylinders in the cubic array, t is the sintering time, t_0 is the fictitious time at which $x = 0$, and l_0 and ρ_0 denote the corresponding quantities at $t = 0$.

For the present study, $\rho_0/\rho_{TH} \simeq 0.2$ is the relative density of the as-deposited particles before sintering treatment. a/l_0 is determined from the initial density, Equation 3. The surface area measured by the BET adsorption technique is $\sim 4.7\,m^2\,g^{-1}$, yielding a value of $a \simeq 0.17\,\mu m$ and hence $l_0 \simeq 1.0\,\mu m$. A value of $\gamma = 280\,erg\,cm^{-2}$ for undoped SiO_2 [9] is used for this analysis as γ generally does not vary significantly with small compositional variations. Thus all parameters except η, the viscosity, in Equation 4a are determined, i.e.

$$K = \frac{4.79 \times 10^6}{\eta}\,P\,sec^{-1}. \quad (4b)$$

It will be shown in the following that η can be calculated from the sintering data.

The integral in Equation 1 can readily be evaluated and expressed in terms of the relative density, ρ/ρ_{TH}, and $K(t-t_0)$, the term to the left of the equation, is a dimensionless parameter. For high densities, the model of glass particles arranged in a cubic array is no longer valid and the relation between ρ/ρ_{TH} and $K(t-t_0)$ is better represented by the sintering model of glass with closed spherical pores [5, 7]. Nevertheless, the sintering model shows that for each experimental density datum, there exists a corresponding parameter, $K(t-t_0)$. The $K(t-t_0)$ values thus obtained are plotted against the actual sintering time, t. For densities $< 95\%$, $K(t-t_0)$ and t are linearly related, and the slope gives K and the intercept gives t_0. These quantities are listed in Table I.

Knowing K, the viscosity, η, can be calculated from Equation 4b. The viscosity data are presented as a function of T^{-1} in Fig. 4. For temperatures between 1000 and 1390° C, the viscosity of SiO_2 glass with 6 wt% B_2O_3 obeys the Arrhenius form and can be expressed as

$$\eta = 14.9 \exp\left(\frac{51.3\,kcal\,mol^{-1}}{RT}\right) P. \quad (5)$$

From the values of K and t_0, which are derived from the experimental data, the dimensionless time, $K(t-t_0)$, can be calculated for each sintering time and temperature. When the relative densities of samples sintered at different temperatures are plotted against their respective dimensionless times, the density data can be represented by the single curve, shown in Fig. 5. The data fit the theoretical model reasonably well in the low-

TABLE I

Temperature (° C)	K (sec^{-1})	η (P)
1000	0.489×10^{-3}	9.8×10^9
1100	2.24×10^{-3}	2.1×10^9
1200	8.75×10^{-3}	0.55×10^9
1390	29.6×10^{-3}	0.16×10^9

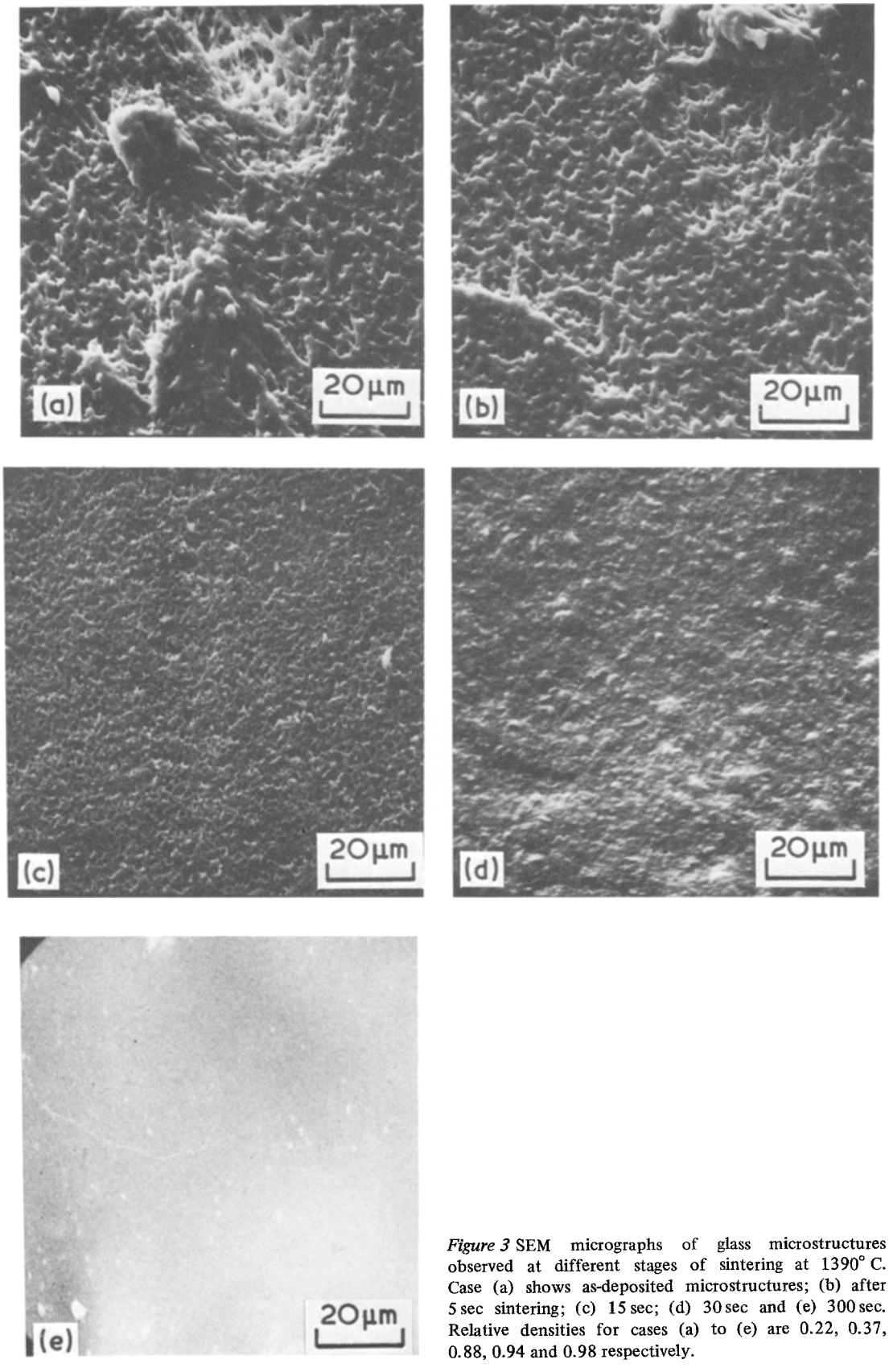

Figure 3 SEM micrographs of glass microstructures observed at different stages of sintering at 1390° C. Case (a) shows as-deposited microstructures; (b) after 5 sec sintering; (c) 15 sec; (d) 30 sec and (e) 300 sec. Relative densities for cases (a) to (e) are 0.22, 0.37, 0.88, 0.94 and 0.98 respectively.

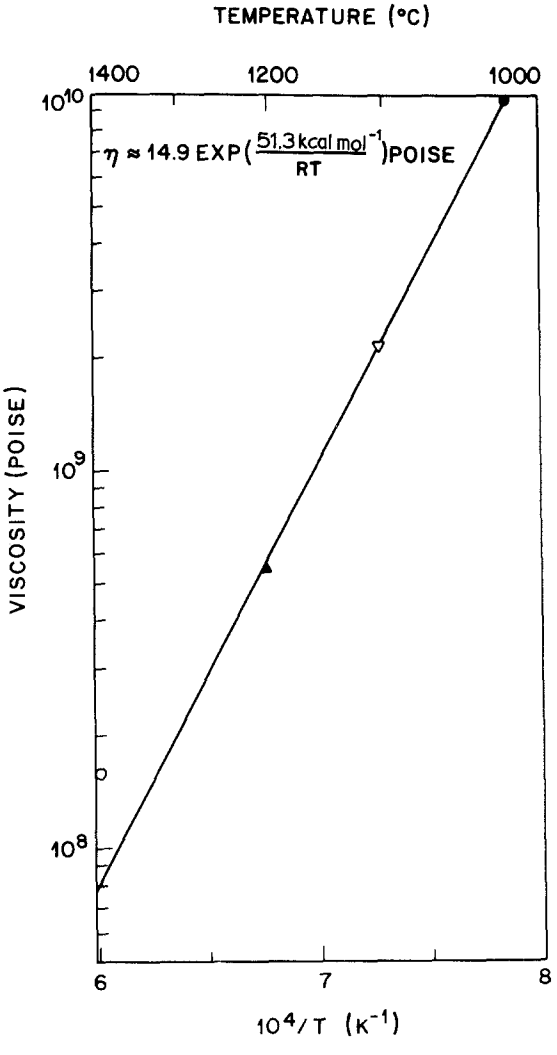

Figure 4 Viscosities, derived from this sintering study of 6% B_2O_3 doped SiO_2, observe the Arrhenius form and can be expressed as $\eta = 14.9 \exp (51.3\ Kcal/RT)$ poise.

TABLE II Viscosity data of borosilicate glasses $\eta = \eta_0 \exp (Q/RT)$

Boron content (wt %)	η_0 (P)	Q (kcal mol^{-1})
0	1.1×10^{-7}	124
3	6.6×10^{-4}	88
6	15	51.3
48	23	33.4

density range. However, in densities >90%, the experimental data gave a low sintered density than predicted by the model.

Viscosity data evaluated from the sintering studies are compared with the published data for SiO_2 [10], borosilicate glasses [10, 11] and B_2O_3 [11], (Fig. 6). The present data are consistent with the published values in this system.

Activation energies of viscosity in these glasses are given in Table II. The values observed in this study follow the trend of decreasing activation energy with increase in the boron content. This is believed to be due to a change in the glass network structure from strongly bonded SiO_4 tetrahedra to an increasing amount of weaker bonded cross-links between boroxyl groups [12]. Furthermore, from the data in Table II, one can make an empirical relation for the viscosity of borosilicates with a boron content, C, by weight,

$$\log \eta = 3.11 - 19.2 \exp(-24C) + \frac{1.68 \times 10^4}{T} + \frac{4.56 \times 10^4 \exp(-22C)}{T}$$

$$0 < C < 0.4 \qquad (6)$$

where η is viscosity in poise and T temperature in K. This empirical relation shows that viscosity is

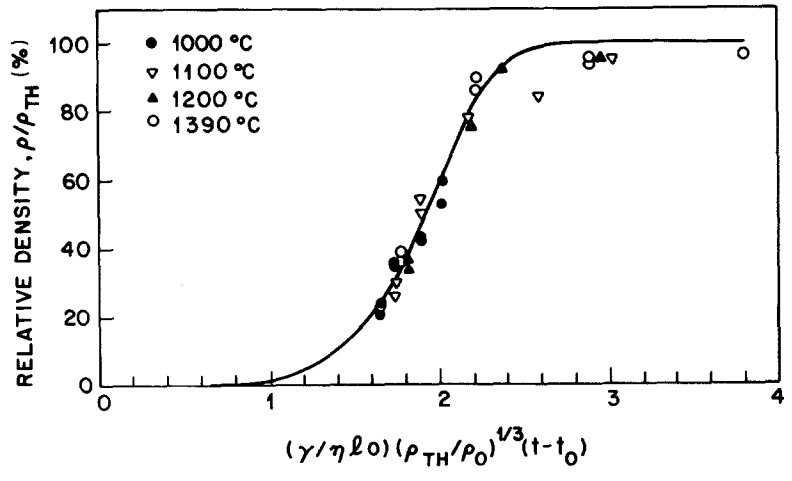

Figure 5 Sintering data, normalized with respect to viscosities at different temperatures, fit the theoretical sintering model reasonably well.

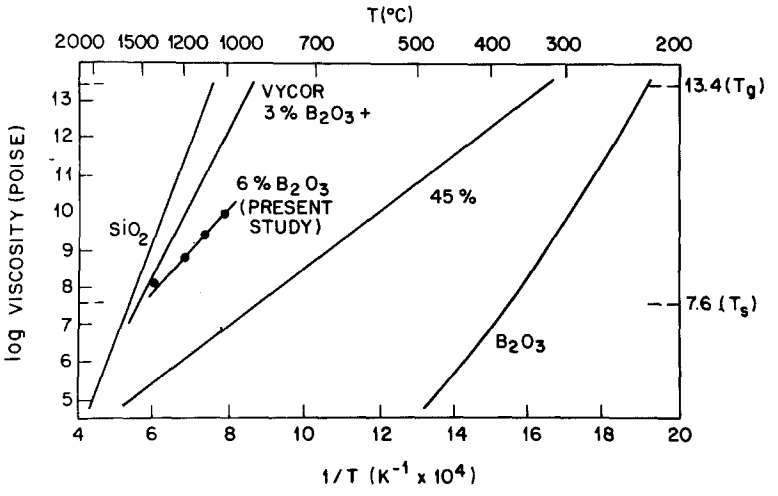

Figure 6 Viscosities derived from this sintering study are shown to be consistent with the published values in the borosilicate glass system.

a function of both temperature and composition. In preform fabrication, changes in composition are usually tailored for optical and other specifications. It is thus desirable to estimate the effect of a compositional change on the sintering temperature in order to achieve the same degree of sintering. Since sintering is controlled by viscous flow, a constant sintering condition implies $d\eta = 0$. From Equation 6,

$$\frac{d\eta}{\eta} = \left[460.8 \exp(-24C) - \frac{1.0 \times 10^6 \exp(-22C)}{T}\right] dC - \left[\frac{4.56 \times 10^4 \exp(-22C)}{T^2} + \frac{1.68 \times 10^4}{T^2}\right] dT. \quad (7)$$

If $d\eta = 0$, then

$$\frac{dT}{dC} = -T^2 \left[\frac{1.0 \times 10^6 \exp(-22C)}{T} - 460.8 \exp(-24C)\right] \Big/ \left[4.56 \times 10^4 \exp(-22C) + 1.68 \times 10^4\right]. \quad (8)$$

This equation shows that an increase in boron content by 1 wt% requires a temperature drop of about 20 to 70° C in order to maintain the same sintering condition. The precise temperature drop required is a function of temperature and composition as shown in Fig. 7. This analysis and a similar one for other dopants should be particularly useful for the fabrication of preform with a graded index which requires a gradual change in the dopant composition.

Bubble growth due to volatile dopants in fibre preforms has been shown to be a serious problem during processing. Since the volatility of dopants usually increases with temperature, the problem of bubble growth can impose an upper limit on the sintering temperature and, therefore, the manufacturing rate of preforms. However, an increase in the dopant content can also lead to a lower sintering temperature and thus a reduced dopant volatility. It is therefore desirable to analyse the net effect of changes in dopant content on the bubble growth problem.

The force balance between the capillary force due to surface tension and the vapour pressure

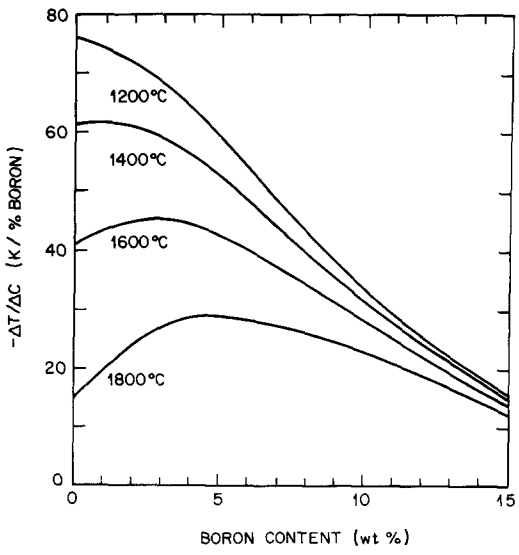

Figure 7 The predicted temperature adjustment required to maintain the same sintering condition after a change in the boron content is graphically expressed as a function of the base line temperature and boron composition.

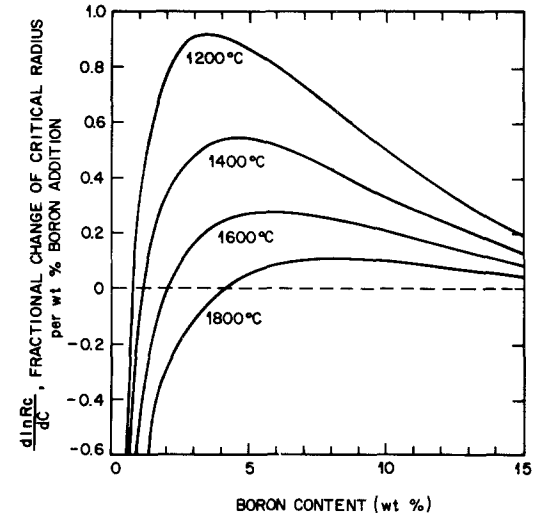

Figure 8 The fractional change of the critical bubble size for a given boron addition is expressed as a function of the base line temperature and boron composition. Proper temperature adjustment to maintain the same sintering condition due to dopant addition is included.

from the volatile dopant gives a critical size above which a bubble can grow catastrophically. The following analysis shows the effect of a compositional change on this critical radius, R_c. The force balance gives

$$\frac{2\gamma}{R_c} = kCp_0 \exp\left(-\frac{\Delta G_v}{RT}\right) \qquad (9)$$

where p_0 and ΔG_v are the pre-exponential term and the activation energy, respectively, of the dopant vapour pressure; and Henry's law for the vapour pressure of a solute in a dilute solution is assumed with a dopant activity coefficient, k, being independent of the dopant concentration. From Equation 9 we get

$$\frac{dR_c}{R_c} = -\left(\frac{1}{C} + \frac{\Delta G_v}{RT^2}\frac{dT}{dC}\right) dC, \qquad (10)$$

for the fractional change in the critical radius due to a compositional variation of the dopant. By substituting Equation 8 for dT/dC into Equation 10, we can calculate the net change in the critical radius for a given change in dopant content while maintaining the same sintering condition. The fractional change of the critical radius depends on the activation energy of dopant vapourization rather than the absolute value of the vapour pressure. Calculations for boron dopant which has a vapourization energy of 77.6 kcal mol^{-1} [13] are shown in Fig. 8. For the case of boron doping, it is interesting to note that at a given temperature there exists a critical composition above which any boron addition may actually help to alleviate the bubble growth problem by increasing the critical bubble radius, i.e. $dR_c/dC > 0$. Based on this analysis, similar calculations can be made for other dopants which may have more serious bubble growth problems.

4. Conclusions

Sintering kinetics of glasses prepared by external vapour deposition technique were quantitatively measured at temperatures ranging from 1000 to 1390° C. Sintering kinetics of borosilicates are consistent with the model proposed for the viscous flow sintering mechanism. The magnitude and the activation energy of the viscosity data derived from the sintering data agree reasonably well with the published viscosity data in the borosilicate system.

From the viscosity data and sintering model, the decrease in sintering temperature per unit change in dopant content is calculated. It is also shown that at a certain compositional range, an increase in the dopant content can actually alleviate the problem of bubble growth while maintaining the same sintering conditions.

This study can be used to determine the relative composition–time–temperature relations for sintering borosilicate glasses. Thus, it has direct applicability to the sintering of soot forms prepared by the external vapour-deposition technique. Furthermore, because of the similarity in microstructures of glasses prepared by the external vapour-deposition and the MCVD processes, one can anticipate similar sintering kinetics for MCVD preforms.

Acknowledgement

The writers thank G. Y. Chin and P. A. Turner for many useful suggestions and critical review of the manuscript, and F. Schrey for the BET surface area analyses.

References

1. J. B. MACCHESNEY, P. B. O'CONNOR and H. M. PRESBY, *Proc. IEEE* **62** (1974) 1278.
2. D. B. KECK, B. FLATS and P. C. SCHULTZ, US Patent no. 3 737 292 (1973).
3. K. L. WALKER, J. W. HARVEY, F. T. GEYLING and S. R. NAGEL, *J. Amer. Ceram. Soc.*, to be published.
4. G. Y SCHERER and D. L. BACHMAN, *J. Amer.*

Ceram. Soc. **60** (1977) 239.
5. G. Y. SCHERER, *ibid.* **60** (1977) 236.
6. J. FRENKEL, *J. Phys. (Moscow)* **9** (1945) 385.
7. J. K. MACKENZIE and R. SHUTTLEWORTH, *Proc. Phys. Soc. London* **62B** (1949) 832.
8. ASTM C373-12, "Standard Method of Test for Water Adsorption, Bulk Density, Apparent Porosity, and Apparent Specific Gravity of Fired Whiteware Products" (1972).
9. N. M. PARIKH, *J. Amer. Ceram. Soc.* **41** (1958) 18.
10. Corning Glass Works Bulletin B-83; "Properties of Selected Commercial Glasses", Corning Glass Works (1949).
11. R. BRUCKNER and F. NAVARRO, *Glastech. Ber.* **39** (1966) 283.
12. R. H. DOREMUS, "Glass Science" (Wiley, New York, 1973) pp. 105–8.
13. J. R. SOULEN, P. STHAPITANONDA and J. L. MARGRAVE, *J. Phys. Chem.* **59** (1955) 132.

Received 21 August and accepted 1 October 1979.